Letter

Thermally induced spin-transfer torques in superconductor/ferromagnet bilayers

I. V. Bobkova,[1,2,3] A. M. Bobkov,[1] and Wolfgang Belzig[4]
[1]Institute of Solid State Physics, Chernogolovka, Moscow Region, 142432 Russia
[2]Moscow Institute of Physics and Technology, Dolgoprudny, 141700 Russia
[3]National Research University Higher School of Economics, Moscow, 101000 Russia
[4]Fachbereich Physik, Universität Konstanz, D-78457 Konstanz, Germany

(Received 10 September 2019; revised 1 December 2020; accepted 17 December 2020; published 11 January 2021)

Thermally induced magnetization dynamics is currently a flourishing field of research due to its potential application in information technology. We study the paradigmatic system of a magnetic domain wall in a thermal gradient which is interacting with an adjacent superconductor. The spin-transfer torques arising in this system due to the combined action of the giant thermoelectric effect and the creation of equal-spin pairs in the superconductor are large enough to give rise to high domain wall velocities 10^3 times larger than previously predicted.

DOI: 10.1103/PhysRevB.103.L020503

Introduction. In recent years a new field of research has emerged by coupling spin and heat degrees of freedom, called spin caloritronics [1]. In particular, the spin Seebeck effect, which is the generation of a spin imbalance by a temperature gradient, has been discussed. Further, a thermally induced spin-transfer torque (STT), based on the spin-dependent Seebeck effect, was predicted and its influence on the domain wall (DW) motion has been discussed [2–9]. There is also experimental evidence of the thermally induced STT in ferromagnetic systems via observations of the magnetization switching and domain wall motion [10–15]. The main mechanisms of the thermal STT are spin transfer via magnons and via thermally induced electron spin flow.

In this Letter, we propose a paradigm of converting thermal gradients to magnetization dynamics in a very efficient and energy saving way. The key idea is to exploit a superconductor/ferromagnet (S/F) hybrid as shown in Fig. 1, where the STT is due to the combined action of the giant thermoelectric effect and creation of equal-spin pairs in the superconductor. Our estimates suggest that domain wall velocities of the order of at least 100 m/s can be achieved by extremely small temperature differences smaller than the critical temperature of conventional low-temperature superconductors such as Al and Nb. The efficiency of the thermal STT can be quantified by the ratio of the domain wall velocity v_{DW} to the temperature gradient ∇T. In principle, our estimates give $v_{DW}/\nabla T \gtrsim 10$–$10^2$ mm^2/K s for the S/F system, which is about three orders of magnitude larger than the values $\sim 10^{-2}$–10^{-1} mm^2/K s reported for thermally induced domain wall motion in ferromagnetic materials [10,12].

In the framework of the discussed mechanism the thermal STT is provided by the electron spin polarization created in *the superconducting part* of the structure and subsequent coupling of this polarization to the ferromagnet magnetization via the exchange mechanism. In principle, the STT is universal and can be relevant for ferromagnetic metals as well as for magnetic insulators. The key ingredient for efficient realization of the thermal STT is the Zeeman splitting of the density of states (DOS) in the superconductor by proximity to the adjacent ferromagnet. The role of the Zeeman splitting is twofold. First, the presence of superconductivity in the system provides a unique mechanism for an antidamping spin-transfer torque, which is not connected to spin-flip scattering of quasiparticles: a superconducting quasiparticle spin cannot align itself to the inhomogeneous magnetization at the length scales shorter than the superconducting coherence length ξ_S because the quasiparticle strongly interacts with the condensate of equal-spin pairs, where the characteristic length scale is ξ_S. Therefore, if the DW width l_{DW} is less than ξ_S, the quasiparticle spins are inevitably misaligned to the DW magnetization giving rise to the nonadiabatic torque.

The second contribution to the STT is the thermally induced quasiparticle spin flow in the superconducting part (spin-dependent Seebeck effect). This quasiparticle spin flow is known to result in the thermal STT in nonsuperconducting systems [2–9]. At the same time a Zeeman-split superconductor is a unique example of a physical system, in which a very large spin Seebeck effect can be realized at low temperatures. The spin Seebeck effect can be quantified in terms of the spin thermopower $\nabla \mu_s/2e\nabla T$ generated by the temperature gradient ∇T in an open circuit, where $\mu_s = \mu_\uparrow - \mu_\downarrow$ is the spin imbalance of the spin-dependent chemical potentials. In order to have a nonzero spin Seebeck effect an electron-hole asymmetry at the Fermi level is required [1,16–20]. Typically the corresponding electron-hole asymmetry in metallic ferromagnets is rather small resulting in the predicted spin thermopower $\mu_s/2e\nabla T \sim 10^{-3}$ mV/K for intermetallic interfaces at room temperature [4,21], while a much smaller spin thermopower $\sim 10^{-6}$ mV/K was measured for a ferromagnetic film [20]. In Zeeman-split superconductors a very large thermopower and spin thermopower was predicted [22–33]. The experimental observation of the large thermopower has been reported [34–36]. Upon application of strong in-plane magnetic fields $B \sim 1$ T or by proximity to a magnetic insulator, Seebeck coefficients of the order of 0.3 mV/K were measured, which is comparable to the thermopower measured

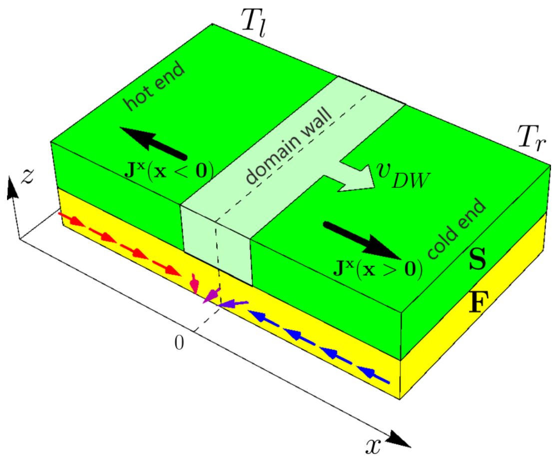

FIG. 1. Sketch of the bilayer S/F system. The magnetization of the ferromagnet F has a form of a head-to-head domain wall (DW) and is indicated by arrows. The picture on the top surface illustrates the process of thermally induced spin pumping into the DW region. Thermally induced quasiparticles both electron- and holelike move from the hot to the cold end. In the bulk of both domains the magnetic moments of the quasiparticles are polarized along the corresponding magnetization. Therefore, the spin current (opposite to the magnetization current) in the bulk of both domains is directed away from the DW. In the left (hotter) domain the direction of the majority spin flow is opposite to the spin current direction, while in the right (colder) domain they coincide. Therefore, the spin current flowing in both domains, pumps majority spins of the hotter domain into the DW region. This leads to the expansion of the hotter domain and, consequently, the DW moves from the hot to the cold end.

in magnetic semiconductors at much higher temperatures [37].

Model and method. The model system that we consider is shown in Fig. 1. It consists of a spin-textured ferromagnet with a spatially dependent magnetization $\boldsymbol{M}(\boldsymbol{r})$ in contact with a spin-singlet superconductor. The superconductor is assumed to be in the ballistic limit. The ferromagnet can be a metal or an insulator. If the thickness of the S film d_S is smaller than the superconducting coherence length ξ_S, the magnetic proximity effect, which is the influence of the adjacent ferromagnet on the S film, can be described by adding the effective exchange field [38–43] $\boldsymbol{h}(\boldsymbol{r}) \sim -\boldsymbol{M}(\boldsymbol{r})$ to the quasiclassical Eilenberger equation, which we use below to treat the superconductor. While in general the magnetic proximity effect is not reduced to the effective exchange only [44–46], in the framework of the present study we neglect other terms which can be viewed as additional magnetic impurities in the superconductor and focus on the effect of the spin texture. The bilayer film is assumed to be connected to equilibrium reservoirs having different temperatures $T_{l,r}$. We neglect all inelastic relaxation processes in the film assuming that its length is shorter than the corresponding relaxation length.

The torque can be calculated starting from the effective exchange interaction between the spin densities on the two sides of the S/F interface:

$$H_{\rm int} = -\int d^2\boldsymbol{r}\, J_{\rm ex} \boldsymbol{S}\boldsymbol{s}, \tag{1}$$

where $\boldsymbol{s}$ is the electronic spin density operator in the S film, $\boldsymbol{S}$ is the localized spin operator in the F film, $J_{\rm ex}$ is the exchange constant, and the integration is performed over the two-dimensional interface. It has been shown [46] that this exchange interaction Hamiltonian results in the appearance of the exchange field $h = J_{\rm ex}M/(2\gamma d_s)$ in the S film. Here M is the saturation magnetization of the ferromagnet and γ is the gyromagnetic ratio.

The spin density $\boldsymbol{s}$ obeys the following equation:

$$\partial_t \boldsymbol{s} = -\partial_j \boldsymbol{J}_j - 2\boldsymbol{h}\times\boldsymbol{s}, \tag{2}$$

where we have introduced the vector $\boldsymbol{J}_j = (J_j^x, J_j^y, J_j^z)$ corresponding to the spin current flowing along the j axis in real space.

The additional contribution to the Landau-Lifshitz-Gilbert equation from the exchange interaction Eq. (1) has the form of a torque acting on the magnetization:

$$\frac{\partial \boldsymbol{M}}{\partial t} = -\gamma \boldsymbol{M}\times\boldsymbol{H}_{\rm eff} + \frac{\alpha}{M}\boldsymbol{M}\times\frac{\partial\boldsymbol{M}}{\partial t} + \frac{J_{\rm ex}}{d_F}\boldsymbol{M}\times\boldsymbol{s}, \tag{3}$$

where α is the Gilbert damping constant and the last term represents the torque. $\boldsymbol{H}_{\rm eff}$ is the local effective field

$$\boldsymbol{H}_{\rm eff} = \frac{H_K M_x}{M}\boldsymbol{e}_x + \frac{2A}{M^2}\nabla^2\boldsymbol{M} - K_\perp M_z \boldsymbol{e}_z. \tag{4}$$

H_K is the anisotropy field, along the x axis, A is the exchange constant, and the self-demagnetization field $K_\perp M_z$ is included.

In a stationary situation $\partial_t \boldsymbol{s} = 0$ from Eq. (2) one can obtain that

$$\boldsymbol{N} = \frac{J_{\rm ex}}{d_F}\boldsymbol{M}\times\boldsymbol{s} = \gamma\frac{d_S}{d_F}\partial_j\boldsymbol{J}_j. \tag{5}$$

The spin current $\boldsymbol{J}_j$ in the superconductor is calculated in the framework of the Keldysh technique for quasiclassical Green's functions. All the technical details of the Green's function calculation are given in the Supplemental Material [47].

To understand the efficiency of the torque $\boldsymbol{N}$ induced by the presence of the superconductor, we compare its value to the characteristic value of the torque induced by the effective field $H_{\rm eff}$. Equation (5) can be rewritten as $\boldsymbol{N}/\gamma H_K M = \zeta\,\partial_{\tilde{x}}\tilde{\boldsymbol{J}}_x$, with the dimensionless quantities $\partial_{\tilde{x}}\tilde{\boldsymbol{J}}_x = (2e^2 R_N v_F/\Delta_0^2)\partial_x \boldsymbol{J}_x$ and $\zeta = E_S/\pi E_A$. The latter is proportional to the ratio of the condensation energy $E_S = N_F\Delta_0^2 d_S/2$ and the anisotropy energy $E_A = MH_K d_F/2$ per unit area of the film in the (x, y) plane. Here and below $R_N = \pi/(2e^2 N_F v_F)$ is the normal state resistance of the film and Δ_0 is the superconducting order parameter of the S film in the absence of the ferromagnet at zero temperature. Taking $E_S \sim d_S \times (10\text{–}10^3)$ erg/cm^3 (for conventional superconductors such as Al and Nb) and $E_A \sim d_F \times 10^5$ erg/cm^3 for Py thin films [63,64] or $E_A \sim d_F \times (10\text{–}10^2)$ erg/cm^3 for YIG thin films [65], we obtain that ζ can vary in a wide range $\zeta \sim (10^{-4}\text{–}10^2)(d_S/d_F)$.

Thermally induced spin current in a homogeneous S/F bilayer. Now we are ready to calculate the thermally induced spin torque in the S/F bilayer. But at first we discuss briefly thermally induced spin current in a S/F bilayer with a *homogeneous* exchange field without a DW because it is a main ingredient of the torque providing the spin pumping into the DW region. Let us apply a temperature difference $T_l - T_r$ to

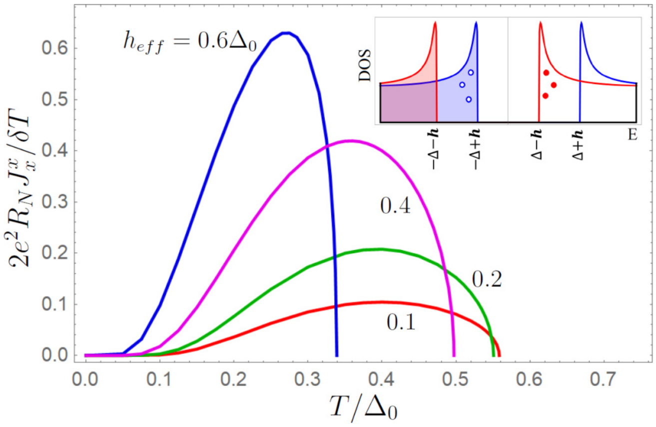

FIG. 2. Spin current divided by the temperature difference $\delta T \to 0$ in the homogeneous S/F bilayer vs the temperature. $h_{\rm eff} = 0.1$ (red), 0.2 (green), 0.4 (purple), and 0.6 (blue) in units of Δ_0. Inset: spin resolved DOS filled by thermally activated right-moving quasiparticles coming from the hot end. The spin-up $S_x = +1$ (spin-down $S_x = -1$) DOS is blue (red). It is seen that all the right-moving quasiparticles contribute to spin flow of the same direction.

the ends of the film. In this case a thermally induced spin current appears in the superconductor. This is a kind of spin Seebeck effect. It is worth noting that the effect does not require an external spin source in the system as opposed to spin pumping experiments in superconductors [66,67]. The spin current in the homogeneous S/F bilayer only carries x-spin component $J_x^x \equiv J$, which is directed along the ferromagnet magnetization. Figure 2 demonstrates the dependence of the spin current on the system temperature at small $\delta T = T_l - T_r \ll T$ for different h. For a homogeneous bilayer the spin thermopower at $\delta T/\Delta_0 \ll 1$ is

$$\frac{2e^2 R_N J}{\delta T} = F\left(\frac{\Delta + h}{2T}\right) - F\left(\frac{\Delta - h}{2T}\right) \tag{6}$$

with $F(x) = x \tanh x - \ln\cosh x$. The maximal values of $2eJR_N/\delta T$ are of the order of $(h/\Delta_0) \times 10^{-1}$ mV/K and are reached for $T \sim 0.6$–$0.7T_c$, as illustrated in Fig. 2.

The estimated values of $2eJR_N/\delta T$ are much larger than those obtained for nonsuperconducting systems containing metallic ferromagnets. Such large values of the spin Seebeck effect are a result of the huge spin-dependent electron-hole asymmetry close to the Fermi level (see the inset of Fig. 2). For the ballistic transport that we consider, the distribution function of right-moving (left-moving) quasiparticles is determined by the Fermi distribution function of the left (right) end of the sample, which is assumed to be in thermal equilibrium at $T = T_{l(r)}$. Let us assume for simplicity that $T_r = 0$. Then there are no left-moving quasiparticles. The spin-split DOS occupied by right-moving quasiparticles is shown in the inset of Fig. 2. We observe that at intermediate temperatures $\Delta - h < T < \Delta + h$ the spin-down DOS is presumably occupied by electronlike quasiparticles, while the spin-up DOS is occupied by holelike quasiparticles. In this ideal situation all the thermally induced quasiparticles (both electrons and holes) have the same spin and contribute to the flow of spin-down quasiparticles to the right, which results in the maximal possible value of the thermally induced spin current.

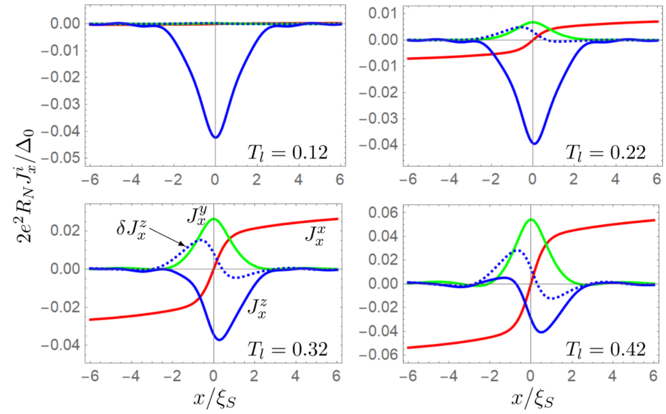

FIG. 3. Spatial profile of the spin current components J_x^x (red), J_x^y (green), and J_x^z (blue) for different temperatures of the hot end, $\delta J_x^z = J_x^z - J_x^z(T_l = T_r)$. $h_{\rm eff} = 0.3\Delta_0$, $T_r = 0.02\Delta_0$, $l_{DW} = 0.5\xi_S$, where $\xi_S = v_F/\Delta_0$ throughout the Letter.

Thermally induced spin-transfer torque. The spatial profiles of the spin current in the presence of a plane DW [located in the (x, y) plane] are presented in Fig. 3 for different temperatures of the hot end. At first, let us focus on the J_x^x component, which is the only nonzero component of the thermally induced spin current in the bulk. Due to the presence of two magnetic domains with opposite magnetizations it leads to spin pumping into the region occupied by the DW. This process is schematically illustrated on the top surface of Fig. 1 and is described there. At nonzero $T_l - T_r$ in-plane component J_x^y also appears in the region of the DW. In the limit $T_l - T_r \to 0$ only J_x^z survives. Then it represents a spontaneous spin current occurring in the region occupied by the wall in equilibrium. It is carried by the equal-spin Cooper pairs generated by the magnetic texture. Similar spontaneous spin currents have already been obtained, usually in a Josephson-junction type geometry [68–76]. The torque generated by this equilibrium spin current is compensated by the DW shape distortion resulting in additional contributions to the in-plane effective field [47]. Consequently, the equilibrium torque contribution does not affect the DW motion and is subtracted from nonequilibrium torque driving the wall.

The torque can be obtained via the spin current according to Eq. (5). In general, any spin torque can be written as $\boldsymbol{N} = a\,\partial_x \boldsymbol{m} + b\,\boldsymbol{m} \times \partial_x \boldsymbol{m}$, where $\boldsymbol{m} = \boldsymbol{M}/M$. The first (second) term can be related to electron spins following (being misaligned to) the magnetic texture. In the framework of the linear response theory the coefficients a and b are proportional to the temperature gradient. For the plane DW under consideration, N_x and N_y components contribute to the adiabatic torque and N_z gives rise to the nonadiabatic contribution.

The temperature dependence of both the adiabatic and the nonadiabatic torques is determined by the spin pumping processes. It closely follows the temperature dependence of the bulk quasiparticle spin current [47]. Therefore, the spin pumping is the driving force of both adiabatic and nonadiabatic torque components. However, it is important to note that in the S/F hybrid the nonadiabatic torque naturally appears because of two different length scales: l_{DW} and ξ_S. A quasiparticle spin is aligned with the magnetization at the

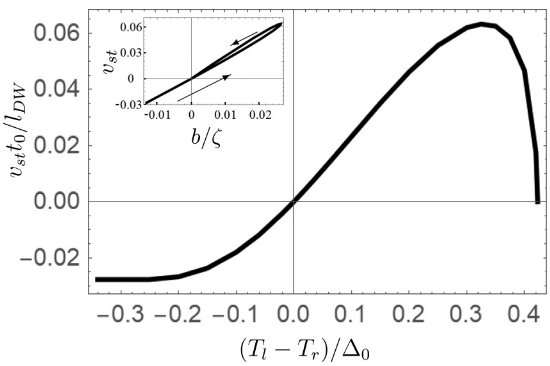

FIG. 4. DW velocity $v_{\rm st}$ as a function of $\delta T = T_l - T_r$. $t_0 = (\gamma H_K)^{-1}$. Inset: $v_{\rm st}$ as a function of $b(x = x_{DW})$. The direction of δT growing along this curve is marked by the arrow. $\zeta = 0.3$, $\alpha = 0.2$, $K_\perp = H_K/M$, $T_r = 0.35\Delta_0$.

length scale $\sim\xi_S$. At $l_{DW} \lesssim \xi_S$ it inevitably mistracks magnetization giving rise to the nonadiabatic torque. The reason is that in the superconductor the quasiparticle is a coherent mixture of electronlike and holelike excitations and strongly interacts with the condensate. Consequently, any changes of the quasiparticle spin are coupled to the changes in the equal-spin condensate wave function, which have characteristic spatial scale ξ_S. This is in contrast to the nonsuperconducting case, where the nonadiabatic torque is believed to be due to spin-flip scattering processes.

Thermally induced DW motion. The dynamics of the DW under the applied temperature difference is calculated from the Landau-Lifshitz- Gilbert equation (3). In the present study we focus on small values of parameter ζ describing how strong is the torque induced by the superconductor. In this case we calculate the torque for the unperturbed DW neglecting the distortion of the DW shape due to its motion. Our numerical results for the spatial profiles of the moving DW are presented in the Supplemental Material [47] and demonstrate that the distortion is indeed very small, therefore justifying the above assumption.

We found that for the values of ζ and $T_l - T_r$ considered in Fig. 4 the DW moves as a rigid object reaching the steady state at a characteristic time $t_d = 1/4\pi\alpha\gamma M$; that is, the Walker's breakdown [77] is not reached in our calculation. For the considered parameters we have found no sign of a precessional motion, which is typical for the motion in the regime after the Walker's breakdown. The DW velocity is calculated as $v(t) = \dot{x}_{DW}(t)$, where $x_{DW}(t)$ is the coordinate of the DW center at a given time and is extracted from the dynamical profiles of the magnetization [47]. The steady state velocity $v_{\rm st} = v(t \to \infty)$ as a function of δT is plotted in Fig. 4. We see that at $\delta T \ll \Delta_0$ the velocity is a linear function of the temperature difference. Although in superconducting systems the microscopically calculated coefficients a and b are spatially dependent (see Supplemental Material [47] for details), $v_{\rm st} \sim b(x = x_{DW}) = -l_{DW} N_z(x = x_{DW})$, as is demonstrated in the inset of Fig. 4. It indicates that in this regime the DW motion is determined by the nonadiabatic torque analogously to the case of nonsuperconducting systems [78]. The "hysteretic behavior" of the parametric plot $v_{\rm st}(b)$ is due to the nonmonotonic dependence of the velocity, as well as $b(x_{DW})$ on δT, which in turn results from the suppression of superconductivity by heating of the film.

The DW velocity $v_{\rm st}$ is linearly proportional to the S/F coupling strength ζ. At $\zeta = 0.3$ and taking material parameters for Py films [64] $H_K \sim 500$ Oe and $l_{DW} \sim 20$ nm or for YIG thin films [65] $H_K \sim 0.5$ Oe and $l_{DW} \sim 1$ μm the maximal DW velocities can be estimated from Fig. 4 as $v_{Py} \sim 0.06(\alpha/\alpha_{Py})(l_{DW}/t_0)_{Py}$, which gives us $v_{Py} \sim 100$ m/s. Analogously, $v_{YIG} \sim 10^3$ m/s. In these estimates we take into account that $v_{\rm st} \sim \alpha^{-1}$ and realistic values of $\alpha_{Py} \sim 0.01$ and $\alpha_{YIG} \sim 10^{-4}$.

Conclusion. In summary, we have predicted and microscopically calculated a thermally induced STT in thin film S/F bilayers containing a DW. It features adiabatic as well as nonadiabatic contributions. The physical mechanism of the torque is a unique feature of superconducting hybrids: it results from (i) the extremely efficient quasiparticle spin pumping into the superconducting region close to the DW provided by the giant Seebeck effect and (ii) strong interaction between quasiparticles and the condensate in the superconductor resulting in the characteristic length scale ξ_S of the quasiparticle spin evolution, which, in its turn, gives rise to a nonadiabatic torque contribution at $l_{DW} \lesssim \xi_S$. We have demonstrated that this torque allows for a high-velocity steady DW motion corresponding to $v \sim 100$ m/s at small temperature differences $\sim$1 K applied at the length of several domain wall widths.

Acknowledgments. This work was financially supported by the Deutsche Forschungsgemeinschaft (DFG) through SFB 767 *Controlled Nanosystems*. The work of A.M.B. and I.V.B. is carried out within the state task of ISSP RAS. I.V.B. also acknowledges the financial support by Foundation for the Advancement of Theoretical Physics and Mathematics BASIS.

[1] G. Bauer, E. Saitoh, and B. J. van Wees, Spin caloritronics, Nat. Mater. **11**, 391 (2012).
[2] L. Berger, Thermal forces on ferromagnetic domain walls, associated with the wall entropy, J. Appl. Phys. **58**, 450 (1985).
[3] S. U. Jen and L. Berger, Thermal domain drag effect in amorphous ferromagnetic materials. I. Theory, J. Appl. Phys. **59**, 1278 (1986).
[4] M. Hatami, G. E. W. Bauer, Q. Zhang, and P. J. Kelly, Thermal Spin-Transfer Torque in Magnetoelectronic Devices, Phys. Rev. Lett. **99**, 066603 (2007).
[5] A. A. Kovalev and Y. Tserkovnyak, Thermoelectric spin transfer in textured magnets, Phys. Rev. B **80**, 100408(R) (2009).
[6] D. Hinzke and U. Nowak, Domain Wall Motion by the Magnonic Spin Seebeck Effect, Phys. Rev. Lett. **107**, 027205 (2011).
[7] P. Yan, X. S. Wang, and X. R. Wang, All-Magnonic Spin-Transfer Torque and Domain Wall Propagation, Phys. Rev. Lett. **107**, 177207 (2011).
[8] K. M. D. Hals, A. Brataas, and G. E. W. Bauer, Thermopower and thermally induced domain wall motion in (Ga, Mn)As, Solid State Commun. **150**, 461 (2010).

[9] S. Moretti, V. Raposo, E. Martinez, and L. Lopez-Diaz, Domain wall motion by localized temperature gradients, Phys. Rev. B **95**, 064419 (2017).

[10] S. U. Jen and L. Berger, Thermal domain drag effect in amorphous ferromagnetic materials. II. Experiments, J. Appl. Phys. **59**, 1285 (1986).

[11] J. Torrejon, G. Malinowski, M. Pelloux, R. Weil, A. Thiaville, J. Curiale, D. Lacour, F. Montaigne, and M. Hehn, Unidirectional Thermal Effects in Current-Induced Domain Wall Motion, Phys. Rev. Lett. **109**, 106601 (2012).

[12] W. Jiang, P. Upadhyaya, Y. Fan, J. Zhao, M. Wang, Li-Te Chang, M. Lang, K. L. Wong, M. Lewis, Y.-T. Lin, J. Tang, S. Cherepov, X. Zhou, Y. Tserkovnyak, R. N. Schwartz, and K. L. Wang, Direct Imaging of Thermally Driven Domain Wall Motion in Magnetic Insulators, Phys. Rev. Lett. **110**, 177202 (2013).

[13] A. J. Ramsay, P. E. Roy, J. A. Haigh, R. M. Otxoa, A. C. Irvine, T. Janda, R. P. Campion, B. L. Gallagher, and J. Wunderlich, Optical Spin-Transfer-Torque-Driven Domain-Wall Motion in a Ferromagnetic Semiconductor, Phys. Rev. Lett. **114**, 067202 (2015).

[14] H. Yu, S. Granville, D. P. Yu, and J.-Ph. Ansermet, Evidence for Thermal Spin-Transfer Torque, Phys. Rev. Lett. **104**, 146601 (2010).

[15] A. Pushp, T. Phung, C. Rettner, B. P. Hughes, See-Hun Yang, and S. S. P. Parkin, Giant thermal spin-torque-assisted magnetic tunnel junction switching, Proc. Natl. Acad. Sci. USA **112**, 6585 (2015).

[16] M. Johnson and R. H. Silsbee, Thermodynamic analysis of interfacial transport and of the thermomagnetoelectric system, Phys. Rev. B **35**, 4959 (1987); M. Johnson, Charge-spin coupling at a ferromagnet-nonmagnet interface, J. Supercond. **16**, 679 (2003).

[17] L. Gravier, S. Serrano-Guisan, F. Reuse, and J.-P. Ansermet, Thermodynamic description of heat and spin transport in magnetic nanostructures, Phys. Rev. B **73**, 024419 (2006); Spin-dependent Peltier effect of perpendicular currents in multilayered nanowires, *ibid.* **73**, 052410 (2006).

[18] K. Uchida, J. Xiao, H. Adachi, J. Ohe, S. Takahashi, J. Ieda, T. Ota, Y. Kajiwara, H. Umezawa, H. Kawai, G. E. W. Bauer, S. Maekawa, and E. Saitoh, Spin Seebeck insulator, Nat. Mater. **9**, 894 (2010).

[19] A. Slachter, F. Bakker, J. Adam, and B. J. van Wees, Thermally driven spin injection from a ferromagnet into a non-magnetic metal, Nat. Phys. **6**, 879 (2010).

[20] K. Uchida, S. Takahashi, K. Harii, W. Koshibae, K. Ando, S. Maekawa, and E. Saitoh, Observation of the spin Seebeck effect, Nature (London) **455**, 778 (2008).

[21] M. Hatami, G. E. W. Bauer, Q. Zhang, and P. J. Kelly, Thermoelectric effects in magnetic nanostructures, Phys. Rev. B **79**, 174426 (2009).

[22] P. Machon, M. Eschrig, and W. Belzig, Nonlocal Thermoelectric Effects and Nonlocal Onsager relations in a Three-Terminal Proximity-Coupled Superconductor-Ferromagnet Device, Phys. Rev. Lett. **110**, 047002 (2013).

[23] M. S. Kalenkov, A. D. Zaikin, and L. S. Kuzmin, Theory of a Large Thermoelectric Effect in Superconductors Doped with Magnetic Impurities, Phys. Rev. Lett. **109**, 147004 (2012).

[24] A. Ozaeta, P. Virtanen, F. S. Bergeret, and T. T. Heikkila, Predicted Very Large Thermoelectric Effect in Ferromagnet-Superconductor Junctions in the Presence of a Spin-Splitting Magnetic Field, Phys. Rev. Lett. **112**, 057001 (2014).

[25] F. Giazotto, J. W. A. Robinson, J. S. Moodera, and F. S. Bergeret, Proposal for a phase-coherent thermoelectric transistor, Appl. Phys. Lett. **105**, 062602 (2014).

[26] M. S. Kalenkov and A. D. Zaikin, Enhancement of thermoelectric effect in diffusive superconducting bilayers with magnetic interfaces, Phys. Rev. B **91**, 064504 (2015).

[27] P. Machon, M. Eschrig, and W. Belzig, Giant thermoelectric effects in a proximity-coupled superconductor-ferromagnet device, New J. Phys. **16**, 073002 (2014).

[28] S. Kawabata, A. Ozaeta, A. S. Vasenko, F. W. J. Hekking, and F. S. Bergeret, Efficient electron refrigeration using superconductor/spin-filter devices, Appl. Phys. Lett. **103**, 032602 (2013).

[29] F. Giazotto, T. T. Heikkila, and F. S. Bergeret, Very Large Thermophase in Ferromagnetic Josephson Junctions, Phys. Rev. Lett. **114**, 067001 (2015).

[30] J. Linder and M. E. Bathen, Spin caloritronics with superconductors: Enhanced thermoelectric effects, generalized Onsager response-matrix, and thermal spin currents, Phys. Rev. B **93**, 224509 (2016).

[31] I. V. Bobkova and A. M. Bobkov, Thermospin effects in superconducting heterostructures, Phys. Rev. B **96**, 104515 (2017).

[32] A Rezaei, A. Kamra, P. Machon, and W. Belzig, Spin-flip enhanced thermoelectricity in superconductor-ferromagnet bilayers, New J. Phys. **20**, 073034 (2018).

[33] F. Aikebaier, M. A. Silaev, T. T. Heikkila, Supercurrent-induced charge-spin conversion in spin-split superconductors, Phys. Rev. B **98**, 024516 (2018).

[34] S. Kolenda, M. J. Wolf, and D. Beckmann, Observation of Thermoelectric Currents in High-Field Superconductor-Ferromagnet Tunnel Junctions, Phys. Rev. Lett. **116**, 097001 (2016).

[35] S. Kolenda, C. Surgers, G. Fischer, and D. Beckmann, Thermoelectric effects in superconductor-ferromagnet tunnel junctions on europium sulfide, Phys. Rev. B **95**, 224505 (2017).

[36] S. Kolenda, P. Machon, D. Beckmann, and W. Belzig, Nonlinear thermoelectric effects in high-field superconductor-ferromagnet tunnel junctions, Beilstein J. Nanotechnol. **7**, 1579 (2016).

[37] Y. Pu, D. Chiba, F. Matsukura, H. Ohno, and J. Shi, Mott Relation for Anomalous Hall and Nernst Effects in $Ga_{1-x}Mn_xAs$ Ferromagnetic Semiconductors, Phys. Rev. Lett. **101**, 117208 (2008).

[38] A. I. Buzdin, Proximity effects in superconductor-ferromagnet heterostructures, Rev. Mod. Phys. **77**, 935 (2005).

[39] L. N. Bulaevskii, A. I. Buzdin, and S. V. Panjukov, The oscillation dependence of the critical current on the exchange field of ferromagnetic metals (F) in Josephson junction S-F-S, Solid State Commun. **44**, 539 (1982).

[40] W. Belzig, A. Brataas, Y. Nazarov, and G. Bauer, Spin accumulation and Andreev reflection in a mesoscopic ferromagnetic wire, Phys. Rev. B **62**, 9726 (2000).

[41] F. S. Bergeret, A. F. Volkov, and K. B. Efetov, Odd triplet superconductivity and related phenomena in superconductor-ferromagnet structures, Rev. Mod. Phys. **77**, 1321 (2005).

[42] T. Tokuyasu, J. A. Sauls, and D. Rainer, Proximity effect of a ferromagnetic insulator in contact with a superconductor, Phys. Rev. B **38**, 8823 (1988).

[43] A. Millis, D. Rainer, and J. A. Sauls, Quasiclassical theory of superconductivity near magnetically active interfaces, Phys. Rev. B **38**, 4504 (1988).
[44] A. Cottet, D. Huertas-Hernando, W. Belzig, and Yu. V. Nazarov, Spin-dependent boundary conditions for isotropic superconducting Green's functions, Phys. Rev. B **80**, 184511 (2009); Erratum: Spin-dependent boundary conditions for isotropic superconducting Green's functions [Phys. Rev. B **80**, 184511 (2009)], **83**, 139901(E) (2011).
[45] M. Eschrig, A. Cottet, W. Belzig, and J. Linder, General boundary conditions for quasiclassical theory of superconductivity in the diffusive limit: Application to strongly spin-polarized systems, New J. Phys. **17**, 083037 (2015).
[46] A. Kamra, A. Rezaei, and W. Belzig, Spin Splitting Induced in a Superconductor by an Antiferromagnetic Insulator, Phys. Rev. Lett. **121**, 247702 (2018).
[47] See Supplemental Material at http://link.aps.org/supplemental/10.1103/PhysRevB.103.L020503 for the technical details of the Green's function calculation and some auxiliary results on the DW equilibrium shape distortion, the self-consistent order parameter, the temperature dependence of the torque, the spatial profiles of the moving DW and spatial dependence of the coefficients a and b, which includes Refs. [48–62,76].
[48] M. Eschrig, Distribution functions in nonequilibrium theory of superconductivity and Andreev spectroscopy in unconventional superconductors, Phys. Rev. B **61**, 9061 (2000).
[49] M. Eschrig, Scattering problem in nonequilibrium quasiclassical theory of metals and superconductors: General boundary conditions and applications, Phys. Rev. B **80**, 134511 (2009).
[50] A. Stern, Berry's Phase, Motive Forces, and Mesoscopic Conductivity, Phys. Rev. Lett. **68**, 1022 (1992).
[51] M. Stone, Magnus force on skyrmions in ferromagnets and quantum Hall systems, Phys. Rev. B **53**, 16573 (1996).
[52] G. E. Volovik, Linear momentum in ferromagnets, J. Phys. C **20**, L83 (1987).
[53] L. Berger, Possible existence of a Josephson effect in ferromagnets, Phys. Rev. B **33**, 1572 (1986).
[54] S. E. Barnes and S. Maekawa, Generalization of Faraday's Law to Include Nonconservative Spin Forces, Phys. Rev. Lett. **98**, 246601 (2007).
[55] R. A. Duine, Spin pumping by a field-driven domain wall, Phys. Rev. B **77**, 014409 (2008).
[56] W. M. Saslow, Spin pumping of current in non-uniform conducting magnets, Phys. Rev. B **76**, 184434 (2007).
[57] Y. Tserkovnyak and M. Mecklenburg, Electron transport driven by nonequilibrium magnetic textures, Phys. Rev. B **77**, 134407 (2008).
[58] S. Zhang and S. S.-L. Zhang, Generalization of the Landau-Lifshitz-Gilbert Equation for Conducting Ferromagnets, Phys. Rev. Lett. **102**, 086601 (2009).
[59] S. A. Yang, G. S. D. Beach, C. Knutson, Di Xiao, Q. Niu, M. Tsoi, and J. L. Erskine, Universal Electromotive Force Induced by Domain Wall Motion, Phys. Rev. Lett. **102**, 067201 (2009).
[60] S. A. Yang, G. S. D. Beach, C. Knutson, Di Xiao, Z. Zhang, M. Tsoi, Q. Niu, A. H. MacDonald, and J. L. Erskine, Topological electromotive force from domain-wall dynamics in a ferromagnet, Phys. Rev. B **82**, 054410 (2010).
[61] D. S. Rabinovich, I. V. Bobkova, A. M. Bobkov, and M. A. Silaev, Resistive State of SFS Josephson Junctions in the Presence of Moving Domain Walls, Phys. Rev. Lett. **123**, 207001 (2019)
[62] D. S. Rabinovich, I. V. Bobkova, and A. M. Bobkov, Electrical response of S-F-TI-S junctions on magnetic texture dynamics, Phys. Rev. B **101**, 054517 (2020)
[63] G. S. D. Beach, C. Nistor, C. Knutson, M. Tsoi, and J. L. Erskine, Dynamics of field-driven domain-wall propagation in ferromagnetic nanowires, Nat. Mater. **4**, 741 (2005).
[64] G. S. D. Beach, C. Knutson, C. Nistor, M. Tsoi, and J. L. Erskine, Nonlinear Domain-Wall Velocity Enhancement by Spin-Polarized Electric Current, Phys. Rev. Lett. **97**, 057203 (2006).
[65] J. Mendil, M. Trassin, Q. Bu, J. Schaab, M. Baumgartner, C. Murer, P. T. Dao, J. Vijayakumar, D. Bracher, C. Bouillet, C. A. F. Vaz, M. Fiebig, and P. Gambardella, Magnetic properties and domain structure of ultrathin yttrium iron garnet/Pt bilayers, Phys. Rev. Materials **3**, 034403 (2019).
[66] Y. Yao, Qi Song, Y. Takamura, J. P. Cascales, W. Yuan, Y. Ma, Yu Yun, X. C. Xie, J. S. Moodera, and W. Han, Probe of spin dynamics in superconducting NbN thin films via spin pumping, Phys. Rev. B **97**, 224414 (2018).
[67] M. Umeda, Y. Shiomi, T. Kikkawa, T. Niizeki, J. Lustikova, S. Takahashi, and E. Saitoh, Spin-current coherence peak in superconductor/magnet junctions, Appl. Phys. Lett. **112**, 232601 (2018).
[68] I. V. Bobkova and Yu. S. Barash, Effects of spin-orbit interaction on superconductor-ferromagnet heterostructures: Spontaneous electric and spin surface currents, Pis'ma Zh. Eksp. Teor. Fiz. **80**, 563 (2004) [JETP Lett. **80**, 494 (2004)].
[69] R. Grein, M. Eschrig, G. Metalidis, and Gerd Schön, Spin-Dependent Cooper Pair Phase and Pure Spin Supercurrents in Strongly Polarized Ferromagnets, Phys. Rev. Lett. **102**, 227005 (2009).
[70] M. Alidoust, J. Linder, G. Rashedi, T. Yokoyama, and A. Sudbo, Spin-polarized Josephson current in superconductor/ferromagnet/superconductor junctions with inhomogeneous magnetization, Phys. Rev. B **81**, 014512 (2010).
[71] Z. Shomali, M. Zareyan, and W. Belzig, Spin supercurrent in Josephson contacts with noncollinear ferromagnets, New J. Phys. **13**, 083033 (2011).
[72] M. Alidoust and K. Halterman, Spontaneous edge accumulation of spin currents in finite-size two-dimensional diffusive spin-orbit coupled SFS heterostructures, New J. Phys. **17**, 033001 (2015).
[73] K. Halterman, O. T. Valls, and C.-T. Wu, Charge and spin currents in ferromagnetic Josephson junctions, Phys. Rev. B **92**, 174516 (2015).
[74] S. Jacobsen, I. Kulagina, and J. Linder, Controlling superconducting spin flow with spin-flip immunity using a single homogeneous ferromagnet, Sci. Rep. **6**, 23926 (2016).
[75] F. Konschelle, I. V. Tokatly, and F. S. Bergeret, Ballistic Josephson junctions in the presence of generic spin dependent fields, Phys. Rev. B **94**, 014515 (2016).
[76] F. Aikebaier, P. Virtanen, and T. Heikkila, Superconductivity near a magnetic domain wall, Phys. Rev. B **99**, 104504 (2019).
[77] N. L. Schryer and L. R. Walker, The motion of 180° domain walls in uniform dc magnetic fields, J. Appl. Phys. **45**, 5406 (1974).
[78] Z. Li, J. He, and S. Zhang, Effects of spin current on ferromagnets, J. Appl. Phys. **99**, 08Q702 (2006).